Numerical analysis of quasiperiodic oscillations with spherical spacetimes

Kuantay Boshkayev,[1,2,*] Orlando Luongo,[1,3,†] and Marco Muccino[1,‡]

[1]*Al-Farabi Kazakh National University, Al-Farabi Avenue 71, 050040 Almaty, Kazakhstan*
[2]*International University of Information Technology, Manas Street 34/1, 050040 Almaty, Kazakhstan*
[3]*Scuola di Scienze e Tecnologie, Università di Camerino, Via Madonna delle Carceri 9, 62032 Camerino, Italy*

(Received 27 December 2022; accepted 22 November 2023; published 15 December 2023)

We numerically test quasiperiodic oscillations using three theoretically motivated models of spacetime, adopting neutron star sources. Then, we compare our findings with a spherically symmetric spacetime inferred from $F(R)$ gravity, with constant curvature, showing that it fully degenerates with our previous metrics that have been adopted in the context of general relativity. To do so, we work out eight neutron stars in low-mass x-ray binary systems and consider a Reissner-Nordström solution plus a de Sitter phase with unspecified sign for the cosmological constant term. In particular, we investigated three hierarchies, i.e., the first dealing with a genuine Schwarzschild spacetime, the second with de Sitter phase whose sign is not fixed *a priori*, and, finally, a Reissner-Nordström spacetime with an additional cosmological constant contribution. We perform Markov chain Monte Carlo analyses, based on the Metropolis-Hastings algorithm and infer 1-σ and 2-σ error bars. For all the sources, we find suitable agreement with spherical solutions with nonzero cosmological constant terms, i.e., with either de Sitter or anti–de Sitter solutions. From our findings, we notice that the existence of topological contribution to the net charge, suggested from $F(R)$ extensions of gravity, seems to be disfavored. Finally, we focus on the physics of the cosmological constant term here involved, investigating physical consequences and proposing possible extensions to improve our overall treatments.

DOI: 10.1103/PhysRevD.108.124034

I. INTRODUCTION

Interest in the physics of black holes (BHs) has recently increased after the detection of gravitational waves [1] and BH shadows [2]. The latter has put a step toward probing BHs in regimes where Einstein's theory may break down. All the above outcomes have strengthened the idea that a possible epoch of "BH precision astronomy" could start [3].

More broadly, by adopting compact objects, instead of BHs only, such as neutron stars (NSs), white dwarfs, etc. as possible sources of new data, one can find evidence about how stars evolve and configure, how gravity behaves in a strong field regime, and, more generally, hints about cosmological epochs in which the aforementioned objects have been formed [4]. Indeed, joint gravitational and electromagnetic observations from NS mergers have provided unprecedented insight into astrophysics, dense matter physics, gravitation, and cosmology [5].

In addition to the above, low-mass x-ray binaries, where at least one compact object is a NS, as well as microquasars, exhibit analogous quasiperiodic oscillations (QPOs) in their x-ray flux [6–8], identified as narrow peaks of excess energy in the corresponding power spectra [9–13]. These peaks are associated with the process of matter accretion into the compact objects; therefore, the investigation of QPOs can reveal the nature of the system under exam and/or direct NS properties and the underlying gravity models [14–19]. Based on the frequency strength, QPOs can be classified as (1) high-frequency QPOs, within the domain of [0.1; 1] kHz or (2) low-frequency QPOs, showing frequencies smaller than 0.1 kHz.

Several models of QPOs exist. Naively, at very high frequencies, the QPO characteristic frequencies appear close to the value of those of the test particle, geodesic epicyclic oscillations around the gravitating compact object, suggesting that the scenario involving the innermost stable circular orbit of test particles could be the most accredited to explain QPO nature[1] [20,21]. While the exact mechanisms behind QPOs are unclear yet and can vary depending on the specific system, several proposed mechanisms have been studied and are still the subject of active

*kuantay@mail.ru
†orlando.luongo@unicam.it
‡muccino@lnf.infn.it

[1]Very likely, the timescales of particle orbital motions near the compact object under exam provides the QPO frequencies.

debate. Some of the mechanisms that have been suggested to explain QPOs include the following:

Beat frequency model. In certain systems, the QPO frequency could be associated with the beat frequency between the frequency of matter orbiting the compact object and a frequency related to the rotation or oscillation of the compact object itself [22,23].

Resonance in accretion disks. QPOs might arise due to resonance effects in the accretion disk [24–26].

Lense-Thirring precession. The Lense-Thirring effect (frame dragging) causes the precession of the accretion disk, which can lead to periodic modulations in the observed emission, resulting in QPOs [27,28].

Disk-Comptonization instabilities. In some cases, QPOs may be associated with oscillations in the Comptonization process, where high-energy photons scatter off hot electrons in the accretion flow, producing x rays. Oscillations in this process can cause variations in the emitted x-ray flux [29–31].

Oscillations excited in toroidal disk. QPOs in such disks are believed to be caused by various physical processes, such as the interaction between the matter in the disk and the strong gravitational field of the compact object [32–35].

Alfvén wave model. QPOs can be induced in the accreted plasma by the magnetic field of a compact object [36–39].

Transition layer disk model. In this model, the millisecond variability in the x-ray emission from low-mass x-ray binaries is explained by means of dynamics of the centrifugal barrier, a hot boundary region around a neutron star [40,41].

Relativistic precession. This model suggests that QPOs arise from motion of inhomogeneities due to accretion mechanisms, say from blobs or vortexes [6–8,42].

Motivated by the fact that general relativity (GR) in a strong gravity regime can be tested by QPOs, we here consider a static spherical configuration provided by three physically distinct cases. The first case assumes a widely consolidated Schwarzschild spacetime, namely, the simplest approach that one can consider; the second case is its natural extension, adding a unfixed sign of cosmological constant energy-momentum term, namely, the Schwarzschild–de Sitter or anti–de Sitter solutions; last, we envisage a (quasi) Reissner-Nordström solution, where the charge is reinterpreted either as electric or topological. We then consider eight sources of NSs in the low-mass x-ray binaries from which we employ the most recent QPO datasets. We thus apply a Markov chain Monte Carlo (MCMC) analysis, deriving the best-fit parameters and the corresponding 1-σ and 2-σ errors, for each involved model, showing the most suitable ones capable of describing the aforementioned sources.

In particular, we notice that, from extended fourth-order gravity, it is possible to recover the form of the three involved spacetimes with a different physical meaning than the one inferred from GR. In extended scenarios, the charge is not given by the external electromagnetic field, but rather it is a topological charge. Even though the two frameworks fully degenerate, considerations about the physics of our findings are discussed in both GR and extended theories of gravity. As a final conclusion, we notice that no charges are expected to be significant in the analyses, whereas the best treatments are those involving Schwarzschild–de Sitter (or anti–de Sitter) spacetimes. Further, evidence for no need of extending gravity, at this level, is also discussed and critically analyzed.

The paper is organized as follows. In Sec. II, we describe QPOs in detail and how to compute them. The proposed spacetimes are reported and the physical motivations behind them are emphasized. In Sec. III, the case of extended theories of gravity, in particular, $F(R)$ paradigms, are discussed. We emphasize the degeneracy between our approaches in GR and the corresponding results obtained in that context. In Sec. IV, we perform MCMC analyses and discuss the physical interpretations of our findings. Further, we argue plausible consequences of our outcomes. Finally, Sec. V summarizes conclusions and perspectives of our work.

II. QUASIPERIODIC OSCILLATION

Evidence for QPOs have been emphasized in the power spectra of the flux from x-ray binary pulsars, and soon after this first discovery, investigations in accretion disks were carried on [43]. Consequently, QPOs point out how to test gravity and, in general, how to argue information from compact objects and more broadly for cosmological purposes [44]. Indeed, current observational data taken from accretion disks around compact objects put tight frequency measures on QPOs, showing which model for astrophysical processes around compact gravitating objects is the most suitable one [45].

In particular, QPOs depend on the background field equations involved through the use of the underlying spacetime. To clarify it better, assuming a given symmetry and a classical field theory that describes gravity, i.e., GR or alternatives to GR, it is possible to infer the spacetime that fulfills the symmetry itself. This spacetime will depend on the free parameters *induced* by the field theory that we are employing. For instance, in the case of the Schwarzschild metric, the free term is a pointlike mass M only, describing the mass singularity or generally the compact object mass that we model through it. Thus, it appears evident that, in order to test a gravitational theory by virtue of QPO data, one first has to fix the spacetime, getting it from prime principles applied to the alternative field equations, and then, second, one can check how to fix the free parameters of the theory itself.

Motivated by the above considerations, we start with a generic spherically symmetric static spacetime composed of three main parameters: (i) a pointlike mass M, (ii) an effective

vacuum energy term that modifies the energy-momentum tensor by adding a constant contribution to the rest energy, and (iii) a possible charge, acting as the net charge contribution provided by the compact object.

We also reinterpret this metric by means of extended fourth-order $F(R)$ theories of gravity, where this metric can represent a viable solution that fully degenerates with GR if one assumes a Reissner-Nordström spacetime with a de Sitter and/or anti–de Sitter nonvanishing term.

A. Theoretical setup

To get the spherically symmetric gravitational field providing both charge and vacuum energy, we adopt a generic static spherically symmetric spacetime by [46]

$$ds^2 = -e^{\nu(r)}dt^2 + e^{\lambda(r)}dr^2 + r^2(d\theta^2 + \sin^2\theta d\phi^2). \quad (1)$$

Fixing $8\pi G = 1$ and having the Einstein equations under the form

$$T_t{}^t = -e^{-\lambda}\left(\frac{1}{r^2} - \frac{\lambda'}{r}\right) + \frac{1}{r^2}, \quad (2a)$$

$$T_r{}^r = -e^{-\lambda}\left(\frac{1}{r^2} + \frac{\nu'}{r}\right) + \frac{1}{r^2}, \quad (2b)$$

$$T_\theta{}^\theta = -\frac{e^{-\lambda}}{2}\left(\nu'' + \frac{\nu'^2}{2} + \frac{\nu' - \lambda'}{r} - \frac{\nu'\lambda'}{2}\right), \quad (2c)$$

$$T_\phi{}^\phi = T_\theta{}^\theta, \quad (2d)$$

where the above T^μ_ν components refer to the energy-momentum tensor, we can get several classes of solutions if $\lambda = -\nu$, including the standard vacuum solution by Schwarzchild, the Reissner-Nordström solution for a charged BH, and, last but not least, the de Sitter solution, corresponding to a uncharged singularity with a constant nonzero contribution to the energy-momentum tensor.

To be more general, assuming the above mathematical structure of our solution, we propose

$$\lambda = -\nu = -\ln\left(1 - \frac{2M}{r} - \Lambda r^2 + \frac{\mathcal{C}}{r^2}\right), \quad (3)$$

giving rise to a charged solution with a vacuum energy term, i.e., with a nonzero constant value entering the energy-momentum tensor. The spacetime therefore reads

$$ds^2 = -\left(1 - \frac{2M}{r} - \Lambda r^2 + \frac{\mathcal{C}}{r^2}\right)dt^2 + \left(1 - \frac{2M}{r} - \Lambda r^2 + \frac{\mathcal{C}}{r^2}\right)^{-1}dr^2 + r^2 d\Omega^2, \quad (4)$$

where M is the source mass, Λ is the cosmological constant term that acts as the energy of the ground state in the energy-momentum tensor, $\mathcal{C}$ is a constant related to the net charge Q that reduces the Reissner-Nordström to $\mathcal{C} \equiv Q^2$, and finally $d\Omega^2 \equiv d\theta^2 + \sin^2\theta d\phi^2$.

We consider three hierarchies of the above metric:

(i) Model 1 with $\Lambda = \mathcal{C} = 0$, leading to the simplest Schwarzschild solution.
(ii) Model 2 with $\mathcal{C} = 0$ but $\Lambda \neq 0$, which turns out to be a de Sitter solution with the sign unspecified[2];
(iii) Model 3 with $\Lambda \neq 0$ and $\mathcal{C} \neq 0$, i.e., the full metric prompted in Eq. (4).

The physical meaning of the above scenarios is explained in the details below.

(1) We consider, in GR, the most general spherically symmetric spacetime, in a static configuration.
(2) We test whether the energy-momentum tensor provides or not a nonvanishing (constant) contribution associated with the compact object.
(3) We explore the possibility that *globally* NS sources exhibit a nonzero net charge, being not perfectly neutral from the outside, as a consequence of $\mathcal{C} \neq 0$.

The main limitations of the above approach are the following:

(a) Commonly speaking, a NS is not perfectly static, but rather it is supposed to rotate.
(b) The sign of Λ is not fixed *a priori*, leaving open the issue of being a de Sitter or an anti–de Sitter framework to describe the energy-momentum tensor.
(c) The NS, in general, locally or globally neutral, may exhibit a nonspecified net charge Q showing slight deviation from the overall neutrality of the star.

Consequently, a more refined approach would include effects of rotation, providing an explanation about the sign of the rest energy, specifying better how the charge is associated with the NS.

It should be noted that rotation is crucial in astrophysical objects and in the processes taking place in their vicinity. In this regard, the inclusion of rotation will make a noticeable change in the structure of compact objects and in the spacetime around them, respectively. The natural generalization of the line element (4), which describes the spacetime around the rotating object, will include angular momentum or, equivalently, the Kerr parameter. However, it should be stressed that the spacetime around compact objects is more complicated with respect to the ones around black holes, due to the infinite number of parameters, which take into account the deformation of a compact object. Only in a static case can both neutron stars and black holes be described by a similar line element. For simplicity, we will not focus on the effects of rotation here.

[2]In other words, we assume that both de Sitter (positive energy) and anti–de Sitter (negative energy) are possible.

However, as a first toy model treatment, we motivate our choice since the standard Schwarzschild metric has been extensively exploited to match the QPO data with encouraging results. So it appears natural to extend first the scenario of static configurations, rather than working out nonstatic frameworks.

B. QPOs from dynamics of test particles

Bearing all the above in mind, we start with the Lagrangian of the test particles,

$$\mathbb{L} = \frac{1}{2} m g_{\mu\nu} \dot{x}^\mu \dot{x}^\nu, \tag{5}$$

in which m is the test particle mass and $x^\mu(\tau)$ are the worldlines. Here, $\dot{x}^\mu = dx^\mu/d\tau$ represents their four-velocities and so, since the metric is static, the conserved quantities are the (specific) energy and angular momentum, namely, $g_{tt}\dot{t} = -\mathcal{E}$ and $g_{\phi\phi}\dot{\phi} = \mathcal{L}$, where $\mathcal{E}$ and $\mathcal{L}$ are the energy and the angular momentum per unit mass of the test particle, respectively. Moreover, we introduce the normalization parameter $\epsilon = g_{\mu\nu}\dot{x}^\mu\dot{x}^\nu$ that describes null geodesics of massless particles for $\epsilon = 0$, whereas it corresponds to massive particles with timelike geodesics for $\epsilon = -1$.

As $m \neq 0$, the equations of motion are

$$\dot{t} = -\frac{\mathcal{E}}{g_{tt}}, \qquad \dot{\phi} = \frac{\mathcal{L}}{g_{\phi\phi}}, \qquad g_{rr}\dot{r}^2 + g_{\theta\theta}\dot{\theta}^2 = V_{\rm eff}, \tag{6}$$

where the effective potential $V_{\rm eff}$ is

$$V_{\rm eff}(r) = -\left(1 + \frac{\mathcal{E}^2 g_{\phi\phi} + \mathcal{L}^2 g_{tt}}{g_{tt} g_{\phi\phi}}\right). \tag{7}$$

For circular orbits in the equatorial plane, one has $\dot{r} = \dot{\theta} = 0$. Thus, the equations for orbital parameters are given as follows:

$$\Omega_\phi = \pm\sqrt{-\frac{\partial_r g_{tt}}{\partial_r g_{\phi\phi}}}, \tag{8a}$$

$$\dot{t} = u^t = \frac{1}{\sqrt{-g_{tt} - g_{\phi\phi}\Omega_\phi^2}}, \tag{8b}$$

$$\mathcal{E} = -\frac{g_{tt}}{\sqrt{-g_{tt} - g_{\phi\phi}\Omega_\phi^2}}, \tag{8c}$$

$$\mathcal{L} = \frac{g_{\phi\phi}\Omega_\phi}{\sqrt{-g_{tt} - g_{\phi\phi}\Omega_\phi^2}}, \tag{8d}$$

where the sign is + (−) for corotating (counterrotating) orbits [47]. The energy and angular momentum for the metric we have adopted are

$$\mathcal{E} = \frac{\mathcal{C} + r(r - r^3\Lambda - 2m)}{r\sqrt{2\mathcal{C} + r(r-3m)}}, \tag{9a}$$

$$\mathcal{L} = \frac{r\sqrt{-\mathcal{C} + mr - r^4\Lambda}}{\sqrt{2\mathcal{C} + r(r-3m)}}. \tag{9b}$$

Thus, the fundamental frequencies of test particles around a compact object are easily computable and they can be converted to seconds, say Hz $\equiv$ s^{-1}, very easily in order to compare them with data.

In the regime of small oscillations, the displacements from equilibrium positions are $r \sim r_0 + \delta r$ and $\theta \sim \pi/2 + \delta\theta$ and thus oscillations occur as

$$\frac{d^2\delta r}{dt^2} + \Omega_r^2 \delta r = 0, \qquad \frac{d^2\delta\theta}{dt^2} + \Omega_\theta^2 \delta\theta = 0, \tag{10}$$

with the frequencies

$$\Omega_r^2 = -\frac{1}{2g_{rr}(u^t)^2}\partial_r^2 V_{\rm eff}(r,\theta)\Big|_{\theta=\pi/2}, \tag{11}$$

$$\Omega_\theta^2 = -\frac{1}{2g_{\theta\theta}(u^t)^2}\partial_\theta^2 V_{\rm eff}(r,\theta)\Big|_{\theta=\pi/2}, \tag{12}$$

for radial and angular oscillations, respectively.

So, adopting our spacetime, we get

$$\Omega_\phi^2 = \frac{m}{r^3} - \frac{\mathcal{C}}{r^4} - \Lambda, \tag{13a}$$

$$\Omega_\theta^2 = \Omega_\phi^2, \tag{13b}$$

$$\Omega_r^2 = \frac{m(r-6m)}{r^4} + \frac{\Lambda(15m-4r)}{r} + \frac{3\mathcal{C}(3m-4r^3\Lambda)}{r^5} - \frac{4\mathcal{C}^2}{r^6}, \tag{13c}$$

where Ω_ϕ represents the particle angular velocity measured by an asymptotic observer placed at infinity.

From the above angular frequencies, we define the Keplerian frequency $f_\phi = \Omega_\phi/(2\pi)$ and the radial epicyclic frequency of the Keplerian motion $f_r = \Omega_r/(2\pi)$. The relativistic precession model identifies the lower QPO frequency $f_{\rm L}$ with the periastron precession, namely, $f_{\rm L} = f_\phi - f_r$, and the upper QPO frequency $f_{\rm U}$ with the Keplerian frequency, namely, $f_{\rm U} = f_\phi$.

TABLE I. Numerical values of ISCO and inner and outer disk radii for each source, computed from best-fit results of Table II. Model 3 appears to be disfavored with respect to model 2, which turns out to be optimal. For two sources, namely, Cir X-1 and 4U1614 + 091, the ISCO of model 3 does not provide physical results.

Source	Model	ISCO (km)	Inner (km)	Outer (km)
Cir X-1	1	19.62	30.79	52.16
	2	16.32	28.84	48.29
	3	⋯	30.39	53.65
GX 5 − 1	1	19.06	21.33	31.70
	2	20.73	22.15	33.35
	3	20.16	21.47	31.93
GX 17 + 2	1	18.32	18.33	22.94
	2	16.01	17.04	21.09
	3	15.89	16.85	20.81
GX 340 + 0	1	18.54	21.52	29.07
	2	18.88	21.71	29.38
	3	18.50	21.15	28.44
Sco X1	1	17.33	17.72	20.98
	2	15.60	16.67	19.58
	3	16.23	17.43	20.64
4U1608 − 52	1	17.29	17.65	21.75
	2	15.82	16.77	20.50
	3	16.83	18.30	22.97
4U1728 − 34	1	15.30	16.06	18.93
	2	13.37	14.91	17.43
	3	14.06	16.35	19.46
4U0614 + 091	1	16.80	16.95	20.05
	2	14.34	15.60	18.30
	3	⋯	17.66	21.45

Another physical quantity that is of great interest is the radius of the innermost circular stable orbit (ISCO) $r_{\rm ISCO}$. It is determined from the following conditions:

$$\frac{d\mathcal{E}}{dr}=0, \qquad \frac{d\mathcal{L}}{dr}=0. \tag{14}$$

For the Schwarzschild spacetime $r_{\rm ISCO}=6M$, for the Reissner-Nordström metric $r_{\rm ISCO}$ is calculated in Ref. [48] and for other solutions $r_{\rm ISCO}$ is cumbersome. Nevertheless, for our three hierarchies, we estimate $r_{\rm ISCO}$ numerically instead of computing it analytically. This choice has been made due to the complexity of $r_{\rm ISCO}$ with the involved metrics. Thus, numerical results are reported in Table I. As a matter of fact, these outcomes certify that model 3 appears mainly disfavored with respect to model 2, in general. Indeed, for two sources (Cir X-1 and 4U1614 + 091) ISCOs become unphysical, in agreement with large mass predictions taken from MCMC analyses, clearly incompatible with current bounds on NS masses.

III. THE CASE OF $F(R)$ THEORIES

The search for departures from GR represents an open challenge for both cosmology and astrophysics [49].

Alternatives to Einstein's gravity can be split into "extended" theories of gravity and "modified" theories of gravity, see, e.g., [50]. We here limit our attention to the extended class of models named $F(R)$, corresponding to analytical functions that extend the Ricci scalar in the gravitational Lagrangian, fulfilling the equivalence principle [51].

We motivate our choice, noting that the most recent *Planck* satellite results seem to indicate that the most suitable inflationary potential is conformally invariant with $F(R)=R+\alpha R^2$, i.e., with the simplest polynomial extension to GR[3] [53].

The gravitational action of $F(R)$ gravity is given by $I=\int d^4x\sqrt{-g}[F(R)/2+\mathcal{L}_m]$, where $F(R)$ is a function of the Ricci scalar R and $\mathcal{L}_m$ is the matter Lagrangian.[4]

The field equations become

$$F_R(R)G_{\mu\nu}=\kappa^2T_{\mu\nu}+\frac{1}{2}g_{\mu\nu}[F(R)-RF_R(R)] + \left(\nabla_\mu\nabla_\nu-g_{\mu\nu}\Box\right)F_R(R), \tag{15}$$

where $F_R(R)\equiv dF(R)/dR$ and $G_{\mu\nu}\equiv R_{\mu\nu}-(1/2)g_{\mu\nu}R$, the Einstein tensor. For $F(R)\to R$, GR is recovered.

Recalling that $R=0$ for spherical vacuum solution in GR, it is noteworthy that $F(R_0)=F_R(R_0)=0$ in $F(R)$ theories, where $R=R_0$ is a real positive or negative constant.

This framework can account for different classes of models and, following Ref. [61] and assuming a convenient $B=B(r)$, we write

$$ds^2=-Bdt^2+\frac{dr^2}{B}+\frac{r^2d\rho^2}{1-k\rho^2}+r^2\rho^2d\phi^2. \tag{16}$$

So, from the above relation, considering the extended field equations, easily one can compute the Ricci scalar curvature that reads

$$R=-B''-\frac{4B'}{r}-\frac{2B}{r^2}+\frac{2k}{r^2}, \tag{17}$$

[3]Alternatively, a Higgs inflation, neglecting the kinetic term during inflation, is equivalent to $F(R)=R+\alpha R^2$ [52].

[4]Those theories may reproduce, although with several drawbacks, the cosmological epochs of inflation and dark energy [54]. However, simpler versions making use of scalar fields in GR seem to be promising examples of unified dark energy models (see, e.g., [55–59]), being consistent with low data [60].

where $B' = \partial_r B$ and $B'' = \partial_{rr} B$. Thus, as $F(R)$ gravity leads to fourth-order differential equations of motion, assuming $R = R_0$, we recover a second-order differential equation whose solution depends upon two integration constants. So, taking the simplest case $R = R_0$ we get

$$B(r) = k - \frac{c_0}{r} + \frac{c_1}{r^2} - \frac{R_0}{12} r^2. \tag{18}$$

A. Degeneracy problem

In the above picture, the free parameters are k, c_0, c_1, and R_0. It appears clear that $c_1 > 0$ provides a (topological) Reissner-Nordström–de Sitter or anti–de Sitter metric, respectively, for $R_0 > 0$ and $R_0 < 0$. In this picture, however, c_1 does not correspond exactly to the charge of an external electric field, but it appears as a consequence of the complexity of the fourth-order theories of gravity that we are considering. To say it differently, c_1 turns out to be an integration constant for the vacuum solution from which we started in $F(R)$ theories.

This spacetime, for $k = 1$, fully recovers the broadly general class of metrics that we have proposed in Eq. (4). There, the net charge is exactly provided by an external electric field, while Λ is here reexpressed by virtue of the constant Ricci scalar R_0. In other words, the two metrics strongly degenerate, albeit the physics associated with them may differ. On the one hand, at large distances, the case $\Lambda \to 0$ immediately provides that $k = 1$ without the need of further cases, $k \neq 1$. So, without losing generality, it appears evident that it can be fixed as $k = 1$, having that the metric can act as a BH, once the event horizon is located for a given real positive value of radius r_H, with $B(r)$ to vanish. On the other hand, the free c_0 term is positive definite in order to avoid repulsive gravity effects [62–65], so that one can conclude

$$k = 1, \tag{19a}$$

$$c_0 = 2M, \tag{19b}$$

$$c_1 = Q^2, \tag{19c}$$

$$R_0 = 12\Lambda, \tag{19d}$$

in order to recover our previous solution.

The scenario with $c_1 > 0$ is equivalent to a topological Reissner-Nordström–de Sitter or anti–de Sitter spacetime. However, a crucial distinction arises as c_1 is not associated with the charge of an external electric field, but solely represents an integration constant inherent to the vacuum solution. The corresponding metric characterizes a BH if we can identify an event horizon where it becomes real and positive, signifying the point where the function $B(r)$ becomes zero. Moreover, the condition that $B'(r_H) > 0$ might be ensured to get a positive temperature and surface gravity. For example, in the case of a spherical geometry with $k = 1$ and neglecting the contribution of the last term in $B(r)$, our solution depicts a black hole when $c_0 > 0$. Additionally, when $c_1 > 0$, the Reissner-Nordström BH exhibits an internal Cauchy horizon with $B'(r_H) < 0$. In this respect, recent researches have demonstrated that such a horizon is prone to instabilities [66]. However, in our scenario, we have the flexibility to select $c_1 < 0$ to avoid the existence of additional positive roots for $B(r)$. A similar analysis can be extended to the topological cases with $k = 0$ or $k = -1$.

An interesting point is also that $R_0 \neq 0$ has no specified sign, leading to a de Sitter or anti–de Sitter solution.[5] However, in GR this appears tricky: choosing anti–de Sitter instead of de Sitter would modify the physics associated with the NS net energy.

Consequently, our outcomes would indicate whether robust departures from the physical expectations of GR can be found by adopting our eight sources and Eq. (4).

IV. MONTE CARLO ANALYSIS AND THEORETICAL DISCUSSION

We perform a MCMC analysis by means of the Metropolis-Hastings algorithm, searching for the best-fit parameters that maximize the log-likelihood,

$$\ln L = -\sum_{k=1}^{N} \left\{ \frac{[f_{\rm L}^k - f_{\rm L}(p, f_{\rm U}^k)]^2}{2(\sigma f_{\rm L}^k)^2} + \ln(\sqrt{2\pi}\sigma f_{\rm L}^k) \right\}, \tag{20}$$

with N data for each source, sampled as lower frequencies $f_{\rm L}^k$, attached errors $\sigma f_{\rm L}^k$, and upper frequencies $f_{\rm U}^k$. The theoretically computed frequencies, denoted as $f_{\rm L}(p, f_{\rm U}^k)$, also depend on combinations of the parameters p, where p includes M, R_0, and $\mathcal{C}$. This dependence varies according to the specific scenario under consideration.

We modify the Wolfram *Mathematica* code from Ref. [67] and adapt it to the case of QPO data, computing the widest possible parameter spaces over the free coefficients of our metric.[6] In particular, we consider the following priors over the coefficients:

$$M \in [0; 5] M_\odot, \tag{21a}$$

$$R_0 \in [-50; 50] \times 10^{-5}\ \text{km}^{-2}, \tag{21b}$$

$$\mathcal{C} \in [-60; 60]\ \text{km}^2. \tag{21c}$$

[5] In extended theories of gravity, this appears easier to account for as one needs anti–de Sitter with $R_0 < 0$, choosing $k = -1$. This would preserve the metric signature. In GR, a different sign of Λ implies different properties of the ground state energy.

[6] Several applications of this code in cosmology, with different log-likelihoods, have been performed, e.g., in Refs. [68–71].

For each source we perform:

(i) three MCMC analyses for each hierarchy;
(ii) the computation of the log-likelihood from $\mathcal{N} \simeq 10^5$ total number of iterations;
(iii) the search of the best-fit parameters providing the absolute and real maximum of the log-likelihood;
(iv) contours and statistical analyses of the errors, displayed up to 2-σ confidence levels.

To assess the best-fit model out of the three scenarios derived from the underlying metric, we use the Aikake and the Bayesian Information Criterion, respectively, AIC and BIC [72]. Thus, considering our likelihood function from Eq. (20), we define

$$\mathrm{AIC} = -2\ln L_{\max} + 2p, \tag{22a}$$

$$\mathrm{BIC} = -2\ln L_{\max} + p\ln N, \tag{22b}$$

where $\ln L_{\max}$ is the maximum value of the log-likelihood, p is the number of estimated parameters in the model, and N is the number of the sample size. Recognizing the model with the lowest value of the AIC and BIC tests, say AIC_f and BIC_f, as the fiducial (best-suited) model, the statistical evidence in support of the reference model is underlined by the difference $\Delta\mathrm{AIC}/\Delta\mathrm{BIC} = \mathrm{AIC}/\mathrm{BIC} - \mathrm{AIC}/\mathrm{BIC}_f$. Precisely, when comparing models, the evidence against the proposed model or, equivalently, in favor of the reference model can be naively summarized as follows:

$\Delta\mathrm{AIC}$ and $\Delta\mathrm{BIC} \in [0, 3]$, weak evidence;
$\Delta\mathrm{AIC}$ and $\Delta\mathrm{BIC} \in (3, 6]$, mild evidence;
$\Delta\mathrm{AIC}$ and $\Delta\mathrm{BIC} > 6$, strong evidence.

The results, summarized in Table II, are statistically, observationally, and theoretically analyzed below, for each source. The contour plots of the best-suited model parameters are shown in Fig. 1. For each source, the fits of the QPO lower f_{L} and upper f_{U} frequencies for the three models considered in this work are shown in Fig. 2.

Cir X-1. Model 3 is strongly preferred over the other ones. However, from model 3 we get only a lower limit on the mass, i.e., $M > 3M_\odot$, which is incompatible with the NS interpretation supported by Ref. [73]. Model 2, instead, performs better than model 1 and provides a well-constrained mass up to 2-σ. In view of these considerations, model 2 is considered the best one. The data points for this source have been taken from Ref. [74].

GX 5-1 [75,76], *GX 17+2* [77], and *GX 340+0* [78]. For these sources, models 2 and 3 provide good fits to the data, with model 2 weakly favored with respect to model 3. However, in all the cases, model 3 does not constrain at all $\mathcal{C}$, being compatible with zero within 1-σ. The only difference is a quite unexpected large value (in modulus) of R_0 for GX $17+2$, while error bars and the corresponding relative errors are all similar. Therefore, being $\mathcal{C} \approx 0$, model 2 can be considered the best fit for these sources.

Sco X1. Models 2 and 3 provide good fits to the data of this source, with model 3 weakly favored with respect to model 2. This source shows intriguing results, since it seems not to exclude *a priori* either a net topological charge or possible deviations from GR due to a large value of R_0 for both models 2 and 3. However, model 3 provides a mass much higher than the range 1.40–1.52$M_\odot$ obtained by modeling optical light curves of Sco X1 [79], whereas the model 2 mass is closer to the above observational range. Therefore, we conclude that model 2 best fits the data of this source. The data points for this source have been taken from Ref. [80].

4U1608-52. In this case, model 3 is mildly preferred over model 2 and provides a NS mass that is considerably higher than (and inconsistent with) $2.07^{+0.25}_{-0.15}M_\odot$, recently taken from QPO data [81]. On the other hand, within 2-σ, the charge parameter $\mathcal{C}$ is consistent with zero and the mass is consistent with the estimate from model 2, which is closer to the above recent finding from QPOs [81]. These considerations lead us to consider model 2 as the best suited to describe the data of 4U1608-52. The data points for this source have been taken from Ref. [82].

4U1728-34. Model 2 is only weakly preferred over model 3. However, model 3 does not constrain at all $\mathcal{C}$, being compatible with zero within 1-σ and, therefore, we conclude that model 2 is the best fit of the source. The data points for this source have been taken from Ref. [83].

4U0614+091. Model 3 is strongly preferred over the other ones, but provides a lower limit on the source mass of $3.5M_\odot$, which is incompatible with the NS interpretation. This value is also incompatible with the above-mentioned finding from QPOs [81]. For this reason, we conclude that a suitable fit for the data is provided by model 2. The data points for this source have been taken from Ref. [84].

Thus, in view of the above, we can summarize our findings as follows:

(i) The best metric is either Schwarzschild–de Sitter or anti–de Sitter for all the sources.
(ii) The Reissner-Nordström term is always (statistically, observationally, or theoretically) disfavored, indicating either no charge contribution or the absence of departures from extension of gravity. Indeed, we anticipate that the combined influence of the magnetic field and rotation will significantly modify r_{ISCO}/M, f_{L}, and f_{U}. This aspect is intriguing since it could impact our findings, suggesting the presence of a nonzero magnetic charge

TABLE II. Best-fit parameters with the associated 1-σ (2-σ) error bars. For each source, the first, second, and third lines list the results of the MCMC fits for model 1, 2, and 3, respectively. ΔAIC and ΔBIC are computed with respect to the reference model, i.e., the model with the highest value of $\ln L_{\max}$.

Source	M $(M_\odot)$	R_0 $(\times 10^{-5}$ km$^{-2})$	$\mathcal{C}$ (km^2)	$\ln L_{\max}$	AIC	BIC	ΔAIC	ΔBIC
Cir X1	$2.224^{+0.029(+0.058)}_{-0.029(-0.058)}$	...	...	-125.84	254	254	117	115
	$1.846^{+0.045(+0.091)}_{-0.045(-0.090)}$	$1.28^{+0.12(+0.23)}_{-0.12(-0.24)}$	...	-70.07	144	145	7	6
	>3.00	$1.17^{+0.12(+0.25)}_{-0.12(-0.24)}$	$37.67^{+0.81(+1.64)}_{-3.50(-14.01)}$	-65.65	137	139	0	0
GX $5-1$	$2.161^{+0.010(+0.020)}_{-0.010(-0.021)}$	...	...	-200.33	403	404	187	186
	$2.397^{+0.019(+0.038)}_{-0.019(-0.038)}$	$-6.46^{+0.48(+0.95)}_{-0.48(-0.95)}$	...	-106.08	216	218	0	0
	$1.96^{+0.78(+1.09)}_{-0.68(-0.91)}$	$-6.03^{+0.50(+0.93)}_{-1.09(-1.96)}$	$-7.10^{+13.7(+20.5)}_{-7.50(-9.0)}$	-105.94	218	221	2	3
GX $17+2$	$2.07678^{+0.0002(+0.0003)}_{-0.0003(-0.0007)}$	...	...	-1819.02	3640	3641	3543	3543
	$1.733^{+0.011(+0.021)}_{-0.011(-0.022)}$	$21.53^{+0.45(+0.91)}_{-0.45(-0.90)}$	...	-46.42	97	98	0	0
	$1.61^{+1.28(+1.32)}_{-0.57(-0.58)}$	$21.13^{+1.52(+2.03)}_{-3.30(-3.82)}$	$-1.54^{+20.34(+21.22)}_{-5.18(-5.30)}$	-46.42	99	100	2	2
GX $340+0$	$2.102^{+0.003(+0.007)}_{-0.003(-0.007)}$	...	...	-130.86	264	264	8	7
	$2.149^{+0.015(+0.030)}_{-0.015(-0.031)}$	$-1.39^{+0.45(+0.89)}_{-0.44(-0.89)}$	...	-126.06	256	257	0	0
	$1.84^{+0.62(+1.28)}_{-0.59(-0.78)}$	$-1.24^{+0.42(+0.84)}_{-0.63(-2.08)}$	$-4.62^{+10.07(+23.59)}_{-6.19(-6.99)}$	-125.95	258	259	2	2
Sco X1	$1.9649^{+0.0005(+0.0011)}_{-0.0005(-0.0011)}$	...	...	-3887.17	7776	7778	7457	7453
	$1.690^{+0.003(+0.007)}_{-0.003(-0.007)}$	$21.77^{+0.24(+0.49)}_{-0.25(-0.49)}$	...	-158.61	321	326	2	1
	$2.229^{+0.005(+0.010)}_{-0.038(-0.161)}$	$21.88^{+0.24(+0.54)}_{-0.22(-0.48)}$	$7.60^{+0.06(+0.09)}_{-0.59(-2.48)}$	-156.42	319	325	0	0
4U1608 $-$ 52	$1.960^{+0.004(+0.007)}_{-0.004(-0.008)}$	...	...	-235.83	474	474	342	340
	$1.728^{+0.014(+0.028)}_{-0.014(-0.028)}$	$17.62^{+0.94(+1.87)}_{-0.94(-1.88)}$	...	-66.14	136	137	4	3
	$3.057^{+0.018(+0.033)}_{-0.152(-2.267)}$	$13.43^{+1.51(+4.25)}_{-0.48(-1.90)}$	$22.19^{+0.46(+0.76)}_{-3.03(-30.11)}$	-63.22	132	134	0	0
4U1728 $-$ 34	$1.734^{+0.003(+0.006)}_{-0.003(-0.006)}$	...	...	-212.61	427	427	353	353
	$1.445^{+0.016(+0.032)}_{-0.016(-0.032)}$	$30.74^{+1.58(+3.15)}_{-1.58(-3.18)}$	...	-35.15	74	74	0	0
	$2.54^{+0.10(+0.11)}_{-1.55(-1.56)}$	$28.23^{+4.79(+6.68)}_{-2.02(-3.66)}$	$15.41^{+1.86(+1.96)}_{-19.45(-19.56)}$	-34.95	76	76	2	2
4U0614 $+$ 091	$1.904^{+0.001(+0.003)}_{-0.001(-0.003)}$	...	...	-842.97	1688	1689	1354	1351
	$1.545^{+0.011(+0.021)}_{-0.011(-0.021)}$	$28.39^{+0.80(+1.59)}_{-0.80(-1.59)}$	...	-188.70	381	384	47	46
	>3.50	$19.67^{+0.55(+1.71)}_{-0.89(-2.34)}$	$33.291^{+0.022(+0.174)}_{-0.537(-2.063)}$	-163.99	334	338	0	0

contribution that does not invalidate model 3, as previously suggested. This issue clearly warrants further investigation. Nevertheless, to maintain focus on our primary research objectives, we have limited our current study to the specific approximations we have made.

In particular, our results may suggest the presence of:

(a) no topological or standard electric charge, showing a global neutrality of NS, i.e., although the local neutrality is not excluded, it seems that globally the compact object does not exhibit effective charge;
(b) an effective constant energy term, acting as a cosmological constant, but with huge orders of difference. This may be interpreted as a constant energy contribution to the net energy of the NS that modifies its stress energy-momentum and is necessary to describe *in toto* the NS.

For the sake of completeness, we cannot avoid discussing possible drawbacks associated with the statistical analyses we performed. In particular, the results may appear weak and/or biased due to the following reasons:

(i) The sign of the effective cosmological constant remains unclear even within the bounds of our experimental constraints. It depends on the analyses conducted on the sources and, in general, does not align with zero. To provide a comprehensive

perspective, it is essential to remember that our overarching objective was to explore deviations from Einstein's gravity, leading to additional terms, including an effective vacuum energy contribution with an unspecified sign. This implies the presence of a net vacuum energy term that predominantly influences large radii and enhances the stability of our fits.

Regarding the sign issue, it is noteworthy that it remains unspecified for only two sources, suggesting that the data or the underlying theoretical framework may be inadequate. A possible spacetime model that incorporates a vacuum energy term is statistically more favored and warrants further investigation. Consequently, model 2, irrespective of the sign assigned to vacuum energy, emerges as the most suitable option for describing these sources.

As a potential insight that can be drawn from our findings, we propose that the class of generalized de Sitter spacetimes should be explored to determine whether the sources establish a well-defined metric with a specific sign for vacuum energy. This will be the focus of our upcoming investigations.

(ii) More sources are needed to confirm or disfavor the above results. The classes of sources, here involved, exhibit different results among them. If the mass values seem to be almost stable and $\lesssim 3M_\odot$; the other terms appear very different among class of source, but similar within the same class.

(iii) The contours in Fig. 1 appear extremely tight, at least for four sources out of eight. The plots in Fig. 2 do not provide fully viable outcomes for all sources, likely as a consequence of the low number of data points present in the corresponding catalogs. This can be responsible for the strange occurrence for that we cannot conclude that either charge or GR extensions are not present. Refined analyses require more data to improve the error bars taken from the above contours.

(iv) The most general involved metric fully degenerates with standard cases of GR. In fact, it is possible to reobtain the same results of fourth-order $F(R)$ theories in GR when the curvature is constant, suggesting that the most suitable benchmark seems to be GR.

(v) Model 2, applied to each class of data points, indicates that there is no consensus on the Λ sign. Even though this appears licit in $F(R)$, in GR it fixes the sign of vacuum energy, i.e., modifies the energy-momentum tensor. Alternatively speaking, the NS sources seem to require a nonzero contribution to energy, but whose sign corresponds to either de Sitter or anti–de Sitter solutions.

Last, but not least, one may draw a tentative conclusion that model 3 appears to be disfavored, in analogy to the common disfavoring of $f(R)$ gravity compared to GR. It is worth noting that investigations into the constraints posed by extended theories of gravity within the Solar System, context of black hole shadows, and inflationary scenarios have not definitively ruled out $f(R)$ models. However, they have placed stringent limits on their viability.

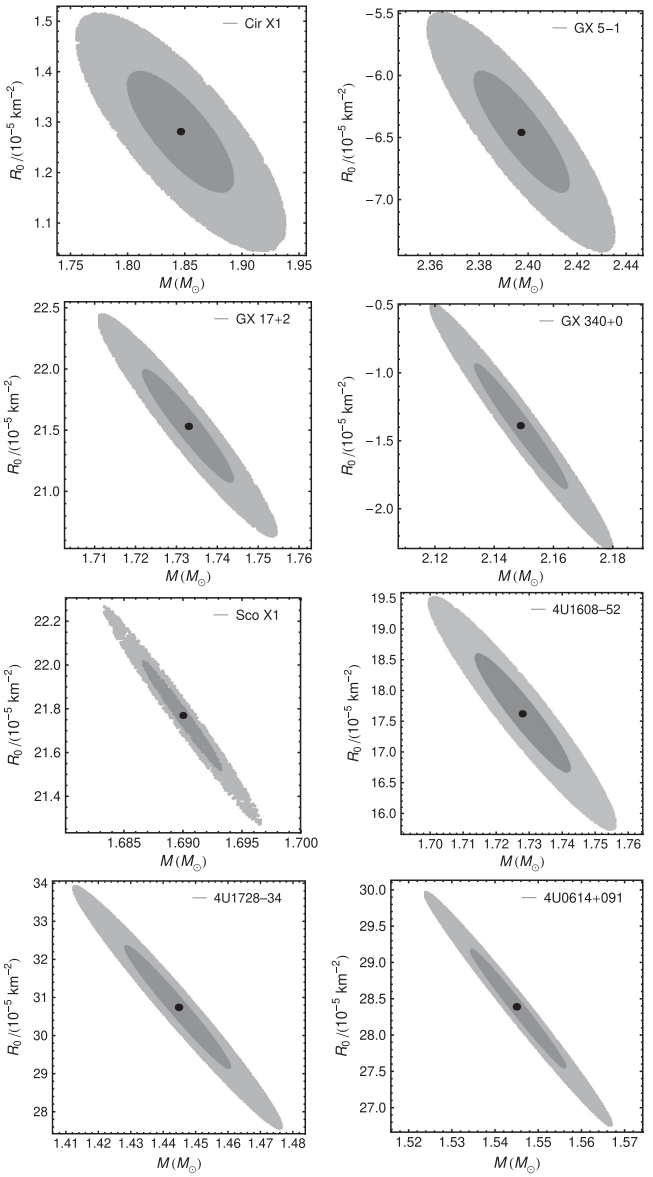

FIG. 1. Contour plots of the best-fit parameters (black dots) and the associated 1-σ (dark gray) and 2-σ (light gray) confidence regions of the sources listed in Table II.

Further, we are operating in regimes of significantly stronger gravity, and the choice of $F(R)$ gravity, along with the corresponding metric derived from it, is expected to shed light on whether $F(R)$ models can effectively account for the observed QPOs. To phrase it differently, if the metric derived from $F(R)$ theories had been conclusively ruled out, it would imply that $F(R)$ models are incapable of accurately describing QPOs. However, our findings,

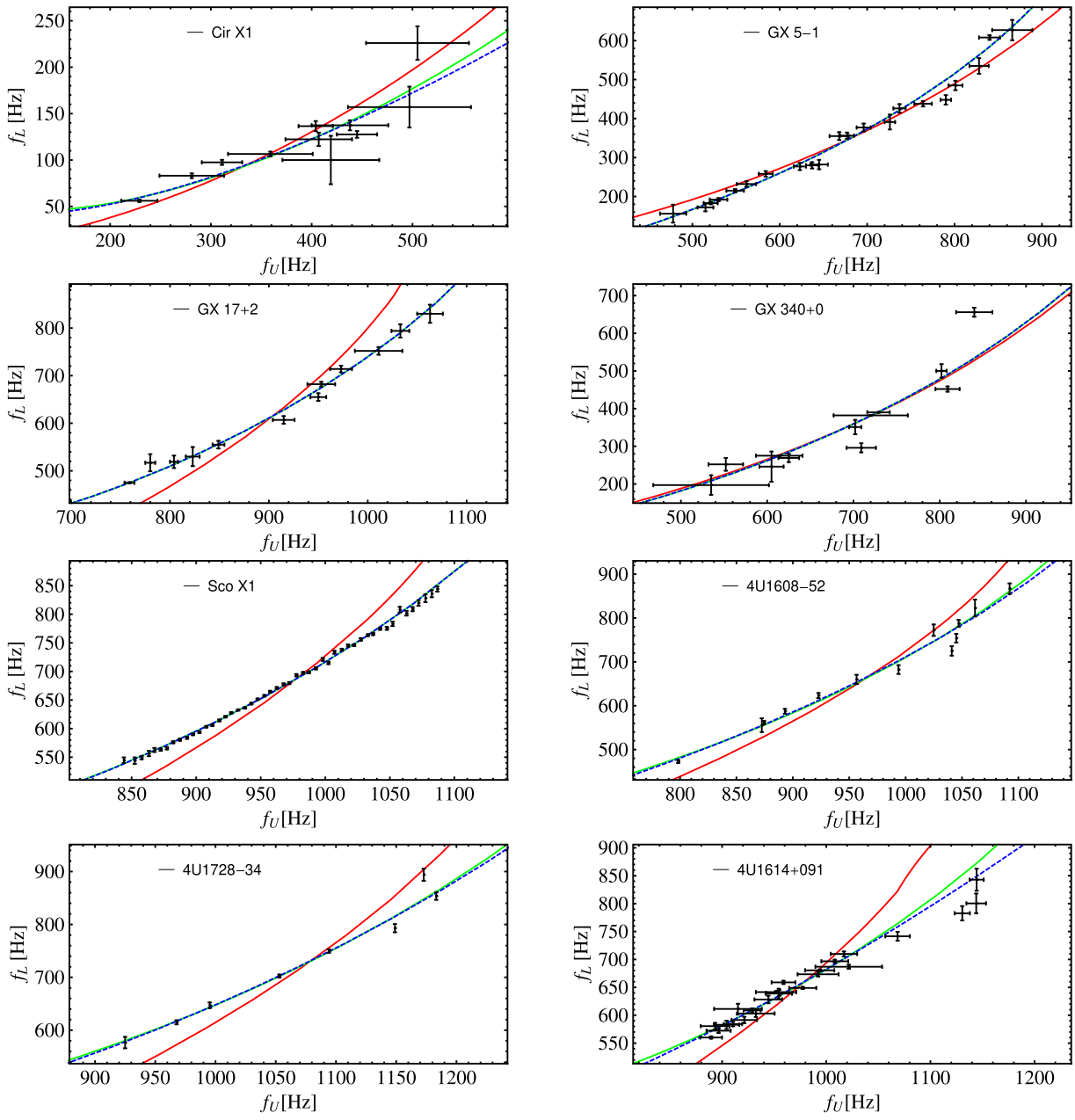

FIG. 2. Fits of the lower frequencies f_{L} vs the upper frequencies f_{U} from the QPO datasets of the sources considered in this work (black data with error bars). Fits have been performed by considering Schwarzschild (red curve), Schwarzschild–de Sitter, or anti–de Sitter (green curve) and Reissner-Nordström (dashed blue curve) spacetimes.

particularly the superior performance of model 2, suggest that both $F(R)$ gravity and GR with a cosmological constant are viable approaches for explaining QPOs.

Remarkably, it is worth noting that the physical significance of Λ is well established within $F(R)$ theories, whereas, in GR, the presence of a cosmological constant might be incorporated by hand into Einstein's energy-momentum tensor.

So, even if the metric degenerates with a spherically symmetric solution in GR, we cannot conclude that model 3 is disfavored because the underlying $F(R)$ background is disfavored.

V. CONCLUSIONS AND PERSPECTIVES

In this paper, we considered eight NS sources and we fitted the corresponding frequency data with three QPO models. In particular, we employed a spherically symmetric static spacetime constructed as a Reissner-Nordström solution with the addition of the de Sitter or anti–de Sitter

contribution. The choice of the metric is discussed in view of both GR and fourth-order extended theories of gravity. Further, we debated the degeneracy between the two frameworks and we stressed that the spacetime describes NSs with a net external charge and a constant term of energy that contributes to the energy-momentum tensor.

The statistical analyses were performed through a MCMC code, based on the Metropolis-Hastings algorithm, that provided best-fit parameters and 1-σ and 2-σ contour plots and error bars. We demonstrated, statistically and theoretically, that the best suite for our results is always represented by the Schwarzschild–de Sitter and anti–de Sitter solutions, though weak evidence in favor of the Reissner-Nordström solution were found.

Given the degeneracy between GR and fourth-order gravity, we demonstrate that all the sources considered here align completely with the predictions of GR and appear to exclude extended gravity theories. However, numerical analyses have not definitively ruled out departures from GR, especially when the curvature is not assumed to be approximately constant, namely, $R = R_0$. Theoretical discussions have advanced in light of the absence of consensus regarding the sign of R_0, which leads to de Sitter and anti–de Sitter phases depending on the specific source under analysis. Furthermore, potential limitations of our approach have also been explored, including the need for more data points and sources.

Further considerations will be investigated in future efforts. In particular, in view of the small number of data points for each source, we can perform mock compilations of data, adopting more refined techniques, e.g., machine learning. Notably, we expect that the combined contribution of the magnetic field and rotation will drastically modify parameters like $r_{\rm ISCO}/M$, $f_{\rm L}$, and $f_{\rm U}$; we intend to check whether this effect could influence our rejecting of model 3. Alternative spacetimes from modified theories of gravity can be also tested, showing whether they could agree with these data and improve the standard fits performed using the Schwarzschild solution. Specifically, further investigations with different spacetimes obtained from $F(R)$ theories, allowing all free parameters to vary, will show whether $F(R)$ models are suppressed in describing QPOs or if there exists the possibility to constrain them with this class of observable. Finally, we will investigate the effects of nonsingular metrics on the overall analysis, checking whether they can improve the quality of our findings.

ACKNOWLEDGMENTS

O. L. is grateful to the Department of Physics of the Al-Farabi University for hospitality during the period in which this manuscript was written. O. L. acknowledges Roberto Giambò for fruitful discussions on the subject of this paper. K. B. acknowledges Mariano Méndez for providing QPO data. K. B. and M. M. acknowledge Grant No. BR21881941, while O. L. acknowledges Grant No. AP19680128, both funded by the Committee of Science at the Ministry of Science and Higher Education of the Republic of Kazakhstan.

[1] B. P. Abbott, R. Abbott, T. D. Abbott, M. R. Abernathy, F. Acernese, K. Ackley, C. Adams, T. Adams, P. Addesso, R. X. Adhikari *et al.*, Phys. Rev. Lett. **116**, 061102 (2016).
[2] K. Akiyama, A. Alberdi, W. Alef, K. Asada, R. Azulay, A.-K. Baczko, D. Ball, M. Baloković, J. Barrett *et al.* (Event Horizon Telescope Collaboration), Astrophys. J. Lett. **875**, L1 (2019).
[3] M. Volonteri, M. Habouzit, and M. Colpi, Nat. Rev. Phys. **3**, 732 (2021).
[4] P. Cerda-Duran and N. Elias-Rosa, Astrophysics and Space Science Library **457**, 1 (2018).
[5] B. P. Abbott, R. Abbott, T. D. Abbott, F. Acernese, K. Ackley, C. Adams, T. Adams, P. Addesso, R. X. Adhikari, V. B. Adya *et al.*, Phys. Rev. Lett. **119**, 161101 (2017).
[6] L. Stella and M. Vietri, Astrophys. J. **492**, L59 (1997).
[7] L. Stella and M. Vietri, Phys. Rev. Lett. **82**, 17 (1999).
[8] L. Stella, M. Vietri, and S. M. Morsink, Astrophys. J. Lett. **524**, L63 (1999).
[9] P. Rebusco, Publ. Astron. Soc. Jpn. **56**, 553 (2004).
[10] M. A. Abramowicz, W. Kluźniak, J. E. McClintock, and R. A. Remillard, Astrophys. J. Lett. **609**, L63 (2004).
[11] G. Török, M. A. Abramowicz, W. Kluźniak, and Z. Stuchlík, Astron. Astrophys. **436**, 1 (2005).
[12] G. Török, P. Bakala, E. Šrámková, Z. Stuchlík, M. Urbanec, and K. Goluchová, Astrophys. J. **760**, 138 (2012).
[13] K. Boshkayev, D. Bini, J. Rueda, A. Geralico, M. Muccino, and I. Siutsou, Gravitation Cosmol. **20**, 233 (2014).
[14] Z. Stuchlik, A. Kotrlova, G. Torok, and K. Goluchova, Acta Astro. **64**, 45 (2014).
[15] K. Boshkayev, J. Rueda, and M. Muccino, Astron. Rep. **59**, 441 (2015).
[16] G. Török, K. Goluchová, M. Urbanec, E. Šrámková, K. Adámek, G. Urbancová, T. Pecháček, P. Bakala, Z. Stuchlík, J. Horák *et al.*, Astrophys. J. **833**, 273 (2016).
[17] K. Boshkayev, J. A. Rueda, and M. Muccino, in *Fourteenth Marcel Grossmann Meeting—MG14*, edited by M. Bianchi, R. T. Jansen, and R. Ruffini (World Scientific, 2018), pp. 3433–3440.
[18] G. Török, K. Goluchová, E. Šrámková, M. Urbanec, and O. Straub, Mon. Not. R. Astron. Soc. **488**, 3896 (2019).
[19] J. Rayimbaev, P. Tadjimuratov, A. Abdujabbarov, B. Ahmedov, and M. Khudoyberdieva, Galaxies **9**, 75 (2021).

[20] M. van der Klis, in *Compact Stellar X-Ray Sources* (Cambridge University Press, Cambridge, England, 2006), Vol. 39, pp. 39–112.
[21] F. K. Lamb and S. Boutloukos, *Accreting Neutron Stars in Low-Mass X-Ray Binary Systems* (Springer Netherlands, Dordrecht, 2008), pp. 87–109, ISBN: 978-1-4020-6544-6.
[22] M. A. Alpar and J. Shaham, Nature (London) **316**, 239 (1985).
[23] F. K. Lamb, N. Shibazaki, M. A. Alpar, and J. Shaham, Nature (London) **317**, 681 (1985).
[24] M. A. Abramowicz and W. Kluźniak, Astron. Astrophys. **374**, L19 (2001).
[25] M. A. Abramowicz, T. Bulik, M. Bursa, and W. Kluźniak, Astron. Astrophys. **404**, L21 (2003).
[26] M. Urbanec, G. Török, E. Šrámková, P. Čech, Z. Stuchlík, and P. Bakala, Astron. Astrophys. **522**, A72 (2010).
[27] A. Ingram, C. Done, and P. C. Fragile, Mon. Not. R. Astron. Soc. **397**, L101 (2009).
[28] L. Stella and A. Possenti, Space Sci. Rev. **148**, 105 (2009).
[29] H. C. Lee and G. S. Miller, Mon. Not. R. Astron. Soc. **299**, 479 (1998).
[30] J. Malzac and R. Belmont, Mon. Not. R. Astron. Soc. **392**, 570 (2009).
[31] J. Poutanen and I. Vurm, Astrophys. J. Lett. **690**, L97 (2009).
[32] L. Rezzolla, S. Yoshida, and O. Zanotti, Mon. Not. R. Astron. Soc. **344**, 978 (2003).
[33] P. J. Montero, L. Rezzolla, and S. Yoshida, Mon. Not. R. Astron. Soc. **354**, 1040 (2004).
[34] O. M. Blaes, E. Šrámková, M. A. Abramowicz, W. Kluźniak, and U. Torkelsson, Astrophys. J. **665**, 642 (2007).
[35] O. Straub and E. Šrámková, Classical Quantum Gravity **26**, 055011 (2009).
[36] C.-M. Zhang, Chin. J. Astron. Astrophys. Suppl. **5**, 21 (2005).
[37] C. M. Zhang, H. X. Yin, Y. H. Zhao, F. Zhang, and L. M. Song, Mon. Not. R. Astron. Soc. **366**, 1373 (2006).
[38] C. M. Zhang, H. X. Yin, Y. H. Zhao, H. K. Chang, and L. M. Song, Astron. Nachr. **328**, 491 (2007).
[39] C. M. Zhang, H. X. Yin, and Y. H. Zhao, Publ. Astron. Soc. Pac. **119**, 393 (2007).
[40] L. Titarchuk, I. Lapidus, and A. Muslimov, Astrophys. J. **499**, 315 (1998).
[41] L. Titarchuk and V. Osherovich, Astrophys. J. Lett. **542**, L111 (2000).
[42] D. Psaltis and C. Norman, arXiv:astro-ph/0001391.
[43] C. Bambi, D. Malafarina, and N. Tsukamoto, Phys. Rev. D **89**, 127302 (2014).
[44] C. Bambi, A. D. Dolgov, and A. A. Petrov, J. Cosmol. Astropart. Phys. 09 (2009) 013.
[45] J. E. McClintock, R. Narayan, S. W. Davis, L. Gou, A. Kulkarni, J. A. Orosz, R. F. Penna, R. A. Remillard, and J. F. Steiner, Classical Quantum Gravity **28**, 114009 (2011).
[46] C. W. Misner, K. S. Thorne, and J. A. Wheeler, *Gravitation* (W. H. Freeman Press, San Francisco, 1973).
[47] C. Bambi and S. Nampalliwar, Europhys. Lett. **116**, 30006 (2016).
[48] D. Pugliese, H. Quevedo, and R. Ruffini, Phys. Rev. D **83**, 024021 (2011).
[49] T. P. Sotiriou and V. Faraoni, Rev. Mod. Phys. **82**, 451 (2010).
[50] T. Clifton, P. G. Ferreira, A. Padilla, and C. Skordis, Phys. Rep. **513**, 1 (2012).
[51] T. P. Sotiriou, Classical Quantum Gravity **23**, 5117 (2006).
[52] D. Y. Cheong, S. M. Lee, and S. C. Park, J. Korean Phys. Soc. **78**, 897 (2021).
[53] A. A. Starobinsky, Phys. Lett. **91B**, 99 (1980).
[54] K. Bamba, S. Capozziello, S. Nojiri, and S. D. Odintsov, Astrophys. Space Sci. **342**, 155 (2012).
[55] S. Capozziello, R. D'Agostino, R. Giambò, and O. Luongo, Phys. Rev. D **99**, 023532 (2019).
[56] K. Boshkayev, R. D'Agostino, and O. Luongo, Eur. Phys. J. C **79**, 332 (2019).
[57] R. D'Agostino, O. Luongo, and M. Muccino, Classical Quantum Gravity **39**, 195014 (2022).
[58] R. D'Agostino and O. Luongo, Phys. Lett. B **829**, 137070 (2022).
[59] O. Luongo and M. Muccino, Phys. Rev. D **98**, 103520 (2018).
[60] A. Aviles, J. Klapp, and O. Luongo, Phys. Dark Universe **17**, 25 (2017).
[61] M. Calzà, M. Rinaldi, and L. Sebastiani, Eur. Phys. J. C **78**, 178 (2018).
[62] O. Luongo and H. Quevedo, in *12th Marcel Grossmann Meeting on General Relativity* (World Scientific, Singapore, 2010), pp. 1029–1031.
[63] O. Luongo and H. Quevedo, Phys. Rev. D **90**, 084032 (2014).
[64] O. Luongo and H. Quevedo, Found. Phys. **48**, 17 (2018).
[65] R. Giambò, O. Luongo, and H. Quevedo, Phys. Dark Universe **30**, 100721 (2020).
[66] R. Myrzakulov and L. Sebastiani, Astrophys. Space Sci. **352**, 281 (2014).
[67] R. Arjona, W. Cardona, and S. Nesseris, Phys. Rev. D **99**, 043516 (2019).
[68] O. Luongo and M. Muccino, Mon. Not. R. Astron. Soc. **503**, 4581 (2021).
[69] O. Luongo and M. Muccino, Astron. Astrophys. **641**, A174 (2020).
[70] M. Muccino, L. Izzo, O. Luongo, K. Boshkayev, L. Amati, M. Della Valle, G. B. Pisani, and E. Zaninoni, Astrophys. J. **908**, 181 (2021).
[71] O. Luongo and M. Muccino, Galaxies **9**, 77 (2021).
[72] A. R. Liddle, Mon. Not. R. Astron. Soc. **377**, L74 (2007).
[73] G. Török, P. Bakala, E. Šrámková, Z. Stuchlík, and M. Urbanec, Astrophys. J. **714**, 748 (2010).
[74] S. Boutloukos, M. van der Klis, D. Altamirano, M. Klein-Wolt, R. Wijnands, P. G. Jonker, and R. P. Fender, Astrophys. J. **653**, 1435 (2006).
[75] R. Wijnands, M. Méndez, M. van der Klis, D. Psaltis, E. Kuulkers, and F. K. Lamb, Astrophys. J. Lett. **504**, L35 (1998).
[76] P. G. Jonker, M. van der Klis, J. Homan, M. Méndez, W. H. G. Lewin, R. Wijnands, and W. Zhang, Mon. Not. R. Astron. Soc. **333**, 665 (2002).
[77] J. Homan, M. van der Klis, P. G. Jonker, R. Wijnands, E. Kuulkers, M. Méndez, and W. H. G. Lewin, Astrophys. J. **568**, 878 (2002).

[78] P. G. Jonker, M. van der Klis, R. Wijnands, J. Homan, J. van Paradijs, M. Méndez, E. C. Ford, E. Kuulkers, and F. K. Lamb, Astrophys. J. **537**, 374 (2000).
[79] A. M. Cherepashchuk, T. S. Khruzina, and A. I. Bogomazov, Mon. Not. R. Astron. Soc. **508**, 1389 (2021).
[80] M. Méndez and M. van der Klis, Mon. Not. R. Astron. Soc. **318**, 938 (2000).
[81] A. Maselli, G. Pappas, P. Pani, L. Gualtieri, S. Motta, V. Ferrari, and L. Stella, Astrophys. J. **899**, 139 (2020).
[82] M. Méndez, M. van der Klis, R. Wijnands, E. C. Ford, J. van Paradijs, and B. A. Vaughan, Astrophys. J. Lett. **505**, L23 (1998).
[83] M. Méndez and M. van der Klis, Astrophys. J. Lett. **517**, L51 (1999).
[84] E. C. Ford, P. Kaaret, K. Chen, M. Tavani, D. Barret, P. Bloser, J. Grindlay, B. A. Harmon, W. S. Paciesas, and S. N. Zhang, Astrophys. J. Lett. **486**, L47 (1997).